The Solution Structures of Mutant Calbindin D_{9k}'s, As Determined by NMR, Show That the Calcium-Binding Site Can Adopt Different Folds†

Charlotta Johansson,*,‡ Magnus Ullner,‡ and Torbjörn Drakenberg‡,§

Physical Chemistry 2, Chemical Center, Lund University, P.O. Box 124, S-22100 Lund, Sweden, and Chemical Laboratory, Technical Research Center of Finland, Biologinkuja 7, P.O. Box 124, SF-02151 Finland

Received March 15, 1993; Revised Manuscript Received April 29, 1993

ABSTRACT: The complete ^{1}H NMR assignments have been obtained for five mutant proteins of calbindin D_{9k} and the three-dimensional solution structures determined for two of the mutants. The structures have been determined using distance geometry and simulated annealing, with distance constraints from NMR. All mutants have modifications in the first calcium-binding site of calbindin (the N-terminal site designated the pseudo-EF-hand). The 3D structure of the mutant with the most extensive modifications in the pseudo-EF-hand shows that the site has turned inside-out and coordinates calcium as in the normal EF-hand (the C-terminal site). In a pseudo-EF-hand loop the calcium is coordinated by main-chain carbonyls, whereas calcium in the normal EF-hand is coordinated by side-chain carboxylates. The 3D structures and ^{1}H NMR assignments show that in order to accomplish a change in the coordinating ligands of the pseudo-EF-hand the loop must be 12 residues long and have glycine in the sixth position. It does, however, seem possible to have alanine instead of aspartic acid in the first calcium coordinating position. The overall global fold of the proteins has not been affected by the mutations in the calcium-binding site, as compared to the wild-type calbindin D_{9k} [Kördel, J., Skelton, N. J., Akke, M., & Chazin, W. J. (1993) *J. Mol. Biol.* (in press)]. The structures consist of two helix-calcium-binding loop-helix motifs, the so called EF-hands, and the loops are connected by a short antiparallel β-sheet. All helices are pairwise in an antiparallel orientation.

The calmodulin super-family contains a large number of different calcium-binding proteins. All of these take part in the regulation of calcium concentrations within cells, which is an important regulatory system used in eucaryotic organisms. Among proteins that belong to this super-family (Strynadka & James, 1989; McPhalen *et al.*, 1991; Nakayama *et al.*, 1992) are calmodulin (CaM; Babu *et al.*, 1985, 1988), troponin C (TnC; Sundralingam *et al.*, 1985; Herzberg & James, 1985), and calbindin D_{9k} (Szebenyi *et al.*, 1981; Szebenyi & Moffat, 1986; Kördel *et al.*, 1993). The proteins have the same calcium-binding motif but participate in largely different events. TnC, for example, is the active calcium-binding protein in the troponin complex and is responsible for triggering muscle contractions, while the role of calbindin D_{9k} in the calcium system is uncertain. Calbindin D_{9k} is the smallest member of this group of proteins known so far (M_w = 8500).

Calbindin D_{9k} has been suggested to act as a transport protein (Kretsinger *et al.*, 1982; Levine & Williams, 1982; Fullmer, 1992) carrying calcium from the cell membrane through the interior of the cells. The suggested action of calbindin as a transport protein and not a regulatory protein is further strengthened by the fact that calbindin undergoes only very subtle changes upon calcium-binding (Skelton *et al.*, 1990). Both TnC and CaM, being calcium dependent regulatory proteins, show significant structural changes upon binding calcium (Herzberg *et al.*, 1986). Calbindin D_{9k} is an ideal protein to study by NMR due to its small size (M_w = 8500), high stability, and the ease by which it can be dissolved to high concentration in an aqueous solution. The protein and many mutants of it have been extensively studied by our group to investigate different biophysical properties following the modifications. We have for example studied a group of mutants with modifications in the calcium-binding loops (Linse *et al.*, 1987; Johansson *et al.*, 1990; Brodin *et al.*, 1990; Johansson *et al.*, 1991), and Linse *et al.* (1991) have investigated the effect of surface charges on calcium-binding. The properties studied have been focused on calcium-binding constants, calcium dynamics, and structural changes.

The highly conserved calcium-binding motif in all of these proteins is called an EF-hand and consists of a 12 amino acid long loop with one α-helix on each side. In the loop the calcium ion is coordinated in a pentagonal bipyramid by seven oxygen ligands (Strynadka & James, 1989), mainly side-chain carboxylates. These helix-loop-helix structures most frequently appear in pairs, but there are cases where one of the sites in the pair does not bind calcium (van Eerd & Takahashi, 1976; Holroyde *et al.*, 1980; Johnson *et al.*, 1980; Wnuk *et al.*, 1984; Luan *et al.*, 1987).

Calbindin D_{9k} consists of two EF-hand motifs, while TnC and CaM have four motifs. The central part of the EF-hand motif, the calcium-binding loop, has amino acids that are the same in almost all of the proteins in the super-family, with some few exceptions (Kretsinger, 1987). The amino acid residues in the C-terminal site (site 2, residues 54–65) of calbindin constitute a normal EF-hand, whereas the N-terminal site (site 1, residues 14–27) is one of the exceptions. In the consensus EF-hand the first amino acid to coordinate calcium in the loop is aspartate, and in the last coordinating position (amino acid number 12) there is a glutamate, which coordinates calcium by both its side-chain oxygens. Furthermore, the sixth amino acid in the loop is glycine in the majority of the EF-hand calcium-binding proteins. This

†This work was supported by grants from the Swedish Natural Science Research Council. The NMR spectrometer was purchased with grants from the Knut and Alice Wallenberg Foundation and the Swedish Council for planning and Coordination of Research. T.D. has been the recipient of a NESTE foundation visiting Scholarship. C.J. acknowledges grants from The Royal Physiographical Society in Lund, The Royal Swedish Academy of Sciences, and NordTek.

* Corresponding author. Present address: Swedish NMR Centre, P.O. Box 17035, S-10462 Stockholm, Sweden.

§Technical Research Center of Finland.

‡Lund University.

0006-2960/93/0432-8429$04.00/0

glycine is important in that it enables the loop to turn, whereby the following amino acids can coordinate calcium by their side chains, and its NH forms a hydrogen bond to the side chain of the aspartate in position 1.

For the N-terminal calcium-binding site (denoted a pseudo-EF-hand; Vogel *et al.*, 1985), however, the loop contains 14 amino acids instead of 12, and some of the invariant amino acids are changed. Aspartate which is normally found in position one of a normal EF-hand is replaced by two alanines and the glycine in position six is replaced by proline + asparagine (Figure 1). These differences render the pseudo-EF-hand an altered fold, since the calcium ion no longer is coordinated predominantly by side-chain carboxylates. Instead the loop has turned itself "inside-out" and coordinates the Ca^{2+} mostly by main-chain carbonyls (Szebenyi *et al.*, 1981; Szebenyi & Moffat, 1986; Kördel *et al.*, 1993). The last coordinating amino acid, a glutamate, still binds calcium through its two side-chain oxygens, but the other calcium ligands are main-chain carbonyls. In spite of these differences the calcium-binding constant is as high in the pseudo-EF-hand as in the normal EF-hand, and calcium-binding occurs in a cooperative manner as calcium-binding within the first or second half of both CaM and TnC (Linse *et al.*, 1987).

In the present work, we have completed ^1H NMR assignments for five mutants of calbindin D_{9k} and calculated the solution structure of two mutant proteins. By stepwise mutations we aimed for the minimum number of mutations in calbindin D_{9k} to accomplish a change in the fold of the pseudo-EF-hand to a normal EF-hand without destroying the calcium-binding ability. The mutants studied here have all been subject to previous biophysical studies, to select mutants for which it is of interest to complete the ^1H NMR assignment and determine the structure. The mutant with the least changes included in this study is P43M. By this mutation cis–trans isomerization of P43 is avoided (Chazin *et al.*, 1989). P43M is included in the study since all mutants have this change, in addition to others, and comparisons of ^1H chemical shifts are made with respect to it. The mutant is similar to the wild-type protein but without cis–trans isomerization. This greatly simplifies the ^1H NMR assignments. Previous biophysical studies of the other mutants of calbindin D_{9k} in the present work include ^{113}Cd, ^{43}Ca, and one-dimensional ^1H NMR as well as determination of the calcium-binding constants (Linse *et al.*, 1987; Johansson *et al.*, 1990; Brodin *et al.*, 1990; Johansson *et al.*, 1991). We are now able to show that in A14Δ+A15D+P20G+N21Δ (defined in Figure 1) the fold of the pseudo-EF-hand has changed into a normal EF-hand fold and the Ca^{2+} affinity is retained, whereas in A15D+P20G the fold of the pseudo-EF-hand is retained.

MATERIALS AND METHODS

Synthesis of the five mutant proteins of calbindin D_{9k} (P43M, A14Δ+P43M, A15D+P20G+P43M, A14Δ+P20G+N21Δ+P43M, and A14Δ+A15D+P20G+N21Δ+P43M) and expression in *Escherichia coli* was performed as reported by Linse *et al.* (1987). The proteins were then purified from the sonicated *E. coli* cells according to Johansson *et al.* (1990).

For the NMR[1] experiments the proteins were dissolved in ^1H_2O containing 10% ^2H_2O for the lock or "100%" ^2H_2O to a protein concentration of 5–6 mM, with no buffer or extra salt added. The samples also contained slightly more than 2 equiv of calcium, making the proteins calcium saturated. pH (not corrected for isotopic effects) was adjusted to 6.0 by microliter additions of 0.01 M NaOH, HCl, NaO^2H, or ^2HCl.

The NMR experiments were performed either on a General Electric Omega 500 spectrometer operating at 500.13 MHz (sample volume 0.43 mL) or on a Varian Unity 600 operating at 599.95 MHz (sample volume 0.70 mL). Standard pulse sequences and phase cycling were utilized to obtain COSY (Marion & Wüthrich, 1983; States *et al.*, 1982), R-COSY (mixing time 30 ms; Wagner, 1983), 2Q (mixing time 30 ms; Braunschweiler *et al.*, 1983), and NOESY (τ_m = 200 ms; Macura & Ernst, 1980) spectra in ^1H_2O or ^2H_2O. TOCSY experiments (spinlock = 120 ms) (Braunschweiler & Ernst, 1983; Bax & Davis, 1985) were performed either using the modification suggested by Rance (1987) and a Dipsi-2 mixing sequence (Shaka *et al.*, 1988) or without these modifications. For the TOCSY and NOESY spectra obtained on the Varian Unity 600 a matched averaging scheme (Ahomäki *et al.*, 1992) was applied where the number of transients changed linearly with t_1. All experiments were obtained at 27 °C, but for some mutant proteins additional COSY and TOCSY spectra at 37 °C were needed to resolve overlapping signals. For the structure calculations NOESY series with the mixing times 20, 40, 80, 100, and 200 ms were obtained, both in ^1H_2O and ^2H_2O.

The carrier was set on the solvent resonance for all experiments (4.75 ppm at 27 °C). A preacquisition delay of 1.2 s was used, and a total of 2048 quadrature pairs of data were collected in hypercomplex mode using either 512 or 256 time increments in t_1. The raw data were processed either on a SUN 360 with GE-Omega software or on a SUN Sparc II using Varian Unity software.

The apodization function used for the COSY, R-COSY, and 2Q spectra was an unshifted sinebell in both t_1 and t_2. In TOCSY and NOESY a shifted squared sinebell was applied prior to Fourier transformation (t_1, 75°; t_2, 60°). All spectra were zerofilled in t_1 to a final data block size 1024 × 2048. In the spin system identification and integration of the NOESY crosspeaks the interactive in-house program MAGNE was used extensively, limiting the need for paper output of spectra.

Spin System Identification. The assignments were performed in two steps. First as many spin systems as possible were identified, and then the sequence specific assignments were obtained, based mainly on $d_{\alpha N}(i,i+1)$ and $d_{NN}(i,i+1)$ NOESY crosspeaks.

The assignment strategy is based on the amide proton shift as described by Chazin *et al.* (1988), whereby the NH/$C^\alpha H$ crosspeak is the starting point, followed by the relayed scalar connectivities for the side-chain protons (Chazin & Wright, 1987; Chazin *et al.*, 1988). Relayed connectivities to the side-chain protons were observed at the backbone NH shift through COSY, R-COSY, and TOCSY spectra acquired in ^1H_2O solution and from the same spectra in ^2H_2O solution starting from the $C^\alpha H$ shift.

For the amino acids with long side chains the spin system identification also started from the end of the side chain. For example the methyl groups in leucine and isoleucine or the $C^\epsilon H_2$ proton in lysine were used as starting points of the identification. This is very similar to the strategy described by Chazin *et al.* (1988).

Identification of the ring proton spin systems for phenylalanine and tyrosine and the side-chain amide groups of

[1] Abbreviations: NMR, nuclear magnetic resonance; COSY, correlation spectroscopy; R-COSY, relayed correlation spectroscopy; TOCSY, total correlation spectroscopy; DIPSI, decoupling in the presence of scalar interactions; NOE, nuclear Overhauser enhancement; NOESY, nuclear Overhauser enhancement and exchange spectroscopy; 2Q, double quantum spectroscopy. The one letter abbreviations for the amino acids are used; for example, A14Δ+P43M, alanine 14 is deleted and proline 43 is replaced by methionine.

asparagine and glutamine residues were made in the aromatic region of the COSY spectrum (approximately 6–8 ppm). This resulted in complete assignments for all residues except F36 and F50. In F50, the aromatic ring proton resonances are almost degenerate, and they also overlap with resonances of F36. Therefore only one chemical shift is given for these protons. For F36 the $C^{\delta}H$ and $C^{\zeta}H$ resonances are degenerate in the mutant P43M. The two resonances found in all other mutants are almost identical to the $C^{\delta}H/C^{\zeta}H$ and $C^{\epsilon}H$ shifts in P43M. Consequently, degeneracy is assumed in all mutant proteins. Assignment is also complicated due to the mentioned overlap with the resonances of F50. Furthermore, one pair of amide protons was left that did not exhibit any characteristic NOEs. These were by default assigned to Q75.

Finally when only one spin system remained, it was by default assigned to the N-terminal methionine, which lacks an NH resonance due to fast exchange of the NH protons with the solvent protons.

Sequence Specific Assignment. The sequential assignments were simplified due to large similarities in chemical shifts between the mutant proteins and the previously assigned P43G mutant (Kördel *et al.*, 1989). Therefore, many of the chemical shifts for each mutant could be obtained directly through a comparison with the chemical shifts of the P43G mutant. However, all sequential assignments were interactively verified by their NOE connectivities in the NOESY spectra. The chemical shifts from the amino acid residues in site I of the mutant proteins, except P43M, differed too much from the corresponding residues in the unmutated calbindin to be obtained by comparison. This was also the case for some other amino acids in the mutants. For these amino acids the sequential assignments were obtained using the normal sequential assignments procedure described in Billeter *et al.* (1982) and Chazin and Wright (1987).

When the complete sequence specific assignment had been carried out through comparison or *de novo*, a new search for missing side-chain assignments was made.

NH Exchange. The exchanges of the amide protons were grouped into three classes: fast, intermediate, and slowly exchanging amide protons. The calcium-loaded protein dissolved in ^1H_2O (pH 6.0) was lyophilized, whereafter it was dissolved in ^2H_2O, and a one-dimensional ^1H NMR spectrum was immediately (approximately 3 min) obtained at 27 °C. The NHs that were missing in this spectrum were classified as fast exchanging. The one-dimensional spectrum was immediately followed by two 8-h NOESY spectra started one after the other. The amide protons present in the first, but not in the second, exchange with an intermediate rate and those present in both spectra are slowly exchanging. The amide proton exchange rate can be used to define the hydrogen bonds, but no hydrogen bonds were included as constraints in the calculations.

Distance Constraints. To determine the interproton distance constraints every peak in the 200-ms NOESY spectrum was evaluated individually. An individually sized box was drawn around every peak defining the integration boundaries. The box size from the 200-ms spectrum was subsequently used to integrate the peaks in all five NOESY spectra (20, 40, 80, 100, and 200 ms). The NOE intensity as a function of mixing time was fitted to a polynomial ($Y = ax^2 + bx + c$) giving a buildup curve from which the slope at $t = 0$ (the initial slope) was used to determine the interproton distance. The initial slope

$$\left.\frac{dN_{ij}}{dt}\right|_{t=0}$$

is proportional to the cross relaxation rate σ_{ij}, which in turn is proportional to $\langle r_{ij}^{-3}\rangle^2$ and τ_{eff}. r_{ij} is the distance between atoms i and j, and τ_{eff} is the effective correlation time. Assuming that τ_{eff} is the same for all interproton vectors we obtain the relationship

$$\frac{r_{ij}}{r_{kl}} = \left(\frac{\sigma_{kl}}{\sigma_{ij}}\right)^{1/6} = \left(\left.\frac{dN_{kl}}{dt}\right|_{t=0} \Big/ \left.\frac{dN_{ij}}{dt}\right|_{t=0}\right)^{1/6}$$

The distance r_{ij} is then given by the quotient of the initial slopes using internal reference distances r_{kl}, between, e.g., two aromatic protons (2.50 Å) or between NH_{i+1} and NH_i in an α-helix (2.8 Å).

The distance range used in the calculations was 1.10× (the obtained r_{ij} distance) as the upper limit and 70% of the upper limit as the lower limit but with a minimum of 1.8 Å. For NOEs involving groups not stereospecifically assigned, a further correction was added to the upper limit of the constraint. This correction was 0.9 Å for methylene groups, 1.0 Å for methyl groups, 1.2 Å for intraresidue constraints to aromatic δ or ϵ protons, 2.0 Å for interresidue distances and intraresidue NH to aromatic δ or ϵ protons, and 2.3 Å for isopropyl groups of valine and leucines.

Dihedral Angle Constraints. From the three bond coupling constant between NH and $C^{\alpha}H$, $^3J_{HN\alpha}$, a range of the allowed dihedral angle ϕ resulted using the Karplus equation (Karplus, 1963; Pardi *et al.*, 1984). $^3J_{HN\alpha}$ coupling constants were measured in a COSY spectrum in H_2O, zero filled to a final size of 1024 × 4096. The line fitting routine from the MAGNE program used to measure the coupling constants finds the exact location of the crosspeak, whereafter the intensities of seven one-dimensional spectra along the ω_2 direction, around the ω_1 coordinate, are added together with the proper sign. This results in an antiphase spectrum. Subsequently two Lorentzian lines with the appropriate signs are adjusted to obtain a least-squares fit to the spectra, and the program reports the difference between the lines as a spin coupling constant. $^3J_{\alpha\beta}$ coupling constants were measured in ω_2 crossections and/or in 2D contour plots on screen, from COSY spectra in ^2H_2O processed as for the $^3J_{HN\alpha}$ determination. $^3J_{HN\alpha} < 5$ Hz indicates an α-helix and the dihedral angle constraint $-80 < \phi < -40$ is introduced in the calculations. On the other hand $^3J_{HN\alpha} > 8$ Hz indicates a β-strand conformation and the constraint is then $-160 < \phi < -80$.

Stereospecific assignments of $C^{\beta}H$ protons and constraints for χ_1 angles are given from $^3J_{\alpha\beta}$ together with NOEs between $C^{\alpha}H$-$C^{\beta}H$ and NH-$C^{\beta}H$ (Wagner *et al.*, 1987). Stereospecific assignments of the β-methylene protons can be obtained only if one of the $^3J_{\alpha\beta}$ is greater than 10 Hz or both are smaller than 5 Hz, provided that the essential NOEs are available. When both coupling constants are small, then both $C^{\beta}H$ are gauche to $C^{\alpha}H$ (denoted g^2g^3, where the numbers denote the β-proton) and the constraint $20° < \chi_1 < 100°$ is included. If one coupling is large and the other small, then the conformation can be either g^2t^3 or t^2g^3 (t = trans, g = gauche), and the constraint $140° < \chi_1 < 220°$ or $-100° < \chi_1 < -20°$ is used, respectively.

Structure Calculations. The structure calculations were performed using the standard protocols in the program XPLOR (Brünger, 1990). In the XPLOR protocol a full distance geometry embedding using all atoms was employed without metrization, followed by simulated annealing and a

refinement step. The standard protocols in dg_full_embed.inp, dgsa.inp, and refine.inp were used for the three steps, respectively. Both the simulated annealing and the last refinement step, which also is a dynamical simulated annealing, start at 2000 K, are cooled down to 100 K, and end with Powell minimization (0 K). Metrization was not used in the distance geometry calculations since it resulted in structures with higher energies and more constraint violations after the last refinement stage. Evaluation of the structures was performed with the in-house program MUMLOOK (M. Ullner and O. Teleman). Several cycles of structure calculations were performed to resolve ambiguities in the experimental data and improve the conformations by incorporation of new distance constraints. Thirty conformations were calculated in each cycle. The total energy and number of violations in each conformation were used as a measure to select the best conformations together with a visual inspection. Approximately 10–15 conformations were accepted from each cycle. Additional constraints were included if they did not violate the distance in the chosen set of conformations.

Most of the stereospecific assignments were obtained from $^3J_{\alpha\beta}$ as described above, but some were added after evaluation of the conformations. When two protons or methyl groups in a pseudogroup were oriented in the same way in all chosen conformations, they were then stereospecifically assigned and incorporated in the next calculation cycle.

RESULTS AND DISCUSSION

In this paper we report on the complete ^{1}H NMR assignments for five mutant proteins of calbindin D_{9k} (P43M, A14Δ+P43M, A15D+P20G+P43M, A14Δ+P20G+N21Δ+P43M, and A14Δ+A15D+P20G+N21Δ+P43M) and the calculated solution structure for two of these mutants (A15D+P20G+P43M and A14Δ+A15D+P20G+N21Δ+P43M). The sequential assignment strategy was that of Wüthrich and co-workers [Billeter *et al.*, 1982; reviewed in Wüthrich (1986)], and the ^{1}H spin systems were identified using the strategy described in Chazin *et al.* (1988) for plastocyanin. The ^{1}H chemical shifts of the mutant P43M (supplementary material) are used as a base for comparison of the chemical shifts with the other mutant proteins, which all contain this mutation in addition to others. When P43 is replaced by M, the cis–trans isomerization of P43 is avoided, and only one set of resonances is detected for all amino acids as for the P43G mutant (Chazin *et al.*, 1989). The P43M mutant is used instead of P43G since it gives us the additional advantage of a CNBr cleavage point in the protein (Finn *et al.*, 1992). The chemical shifts of the P43M mutant closely follow those of P43G, so it is most likely that the structures are identical. Previously Kördel *et al.* (1990) compared the wild-type protein with the P43G mutant and concluded that there are no structural differences between these proteins.

Assignments of the Specific Mutant Proteins. In the following all mutant proteins contain the mutation P43M in addition to the other substitutions and/or deletions.

Kördel *et al.* (1990) have previously compared the ^{1}H NMR spectra of the P43G mutant and the wild-type protein. They found that chemical shift differences $\Delta\delta > 0.04$ ppm are present only in the loop with the mutation. All comparisons of the mutants studied here are made with respect to the P43M mutant, and we have therefore performed a similar comparison between the two mutants P43M and P43G. We find that except for an obvious difference in our referencing of 0.03 ppm, there are no shift differences for the backbone protons of more than ±0.04 ppm, except in the region L40–L46. One exception is that the NH of L32 differs by 0.07 ppm, but we have no explanation for this unexpected difference. The overall small differences in chemical shifts show that the structures of the two mutants P43M and P43G are very similar, and the ^{1}H chemical shifts of P43M can therefore be used in the comparisons among the various mutants in the present study. Furthermore, Kördel *et al.* (1993) have shown that the solution structure of P43G is almost identical to the crystal structure of the wild-type calbindin D_{9k} (Szebenyi & Moffat, 1986). Recently, Svensson *et al.* (1992) have shown that the cis–trans isomerization is present in the crystal structure as in solution, but the effect on the crystal structure can be seen only on the G42 and P43 residues. Thus, the mutant P43M

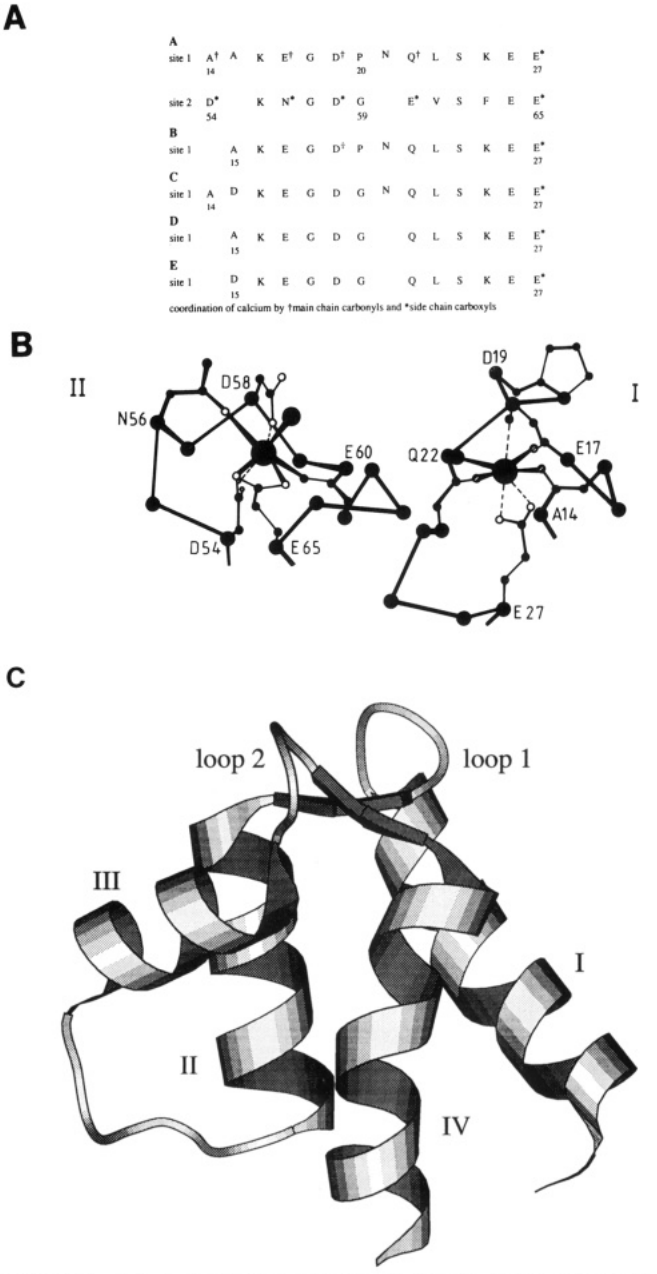

FIGURE 1: (A) Amino acid sequence of the calcium-binding sites in calbindin D_{9k}: A, wild-type calbindin D_{9k}, B, A14Δ+P43M; C, A15D+P20G+P43M; D, A14Δ+P20G+N21Δ+P43M; E, A14Δ+A15D+P20G+N21Δ+P43M. Note that site 2 is left unchanged in the mutant proteins. (B) Backbone representation of the calcium-binding sites in calbindin D_{9k}. The coordinating amino acid residues are marked. Coordinating oxygen atoms indicated with stripes are from backbone carbonyls and those left empty are from side-chain carboxyls. (C) A schematic drawing of calbindin D_{9k} (drawn using Molscript; P. J. Kraulis, 1991).

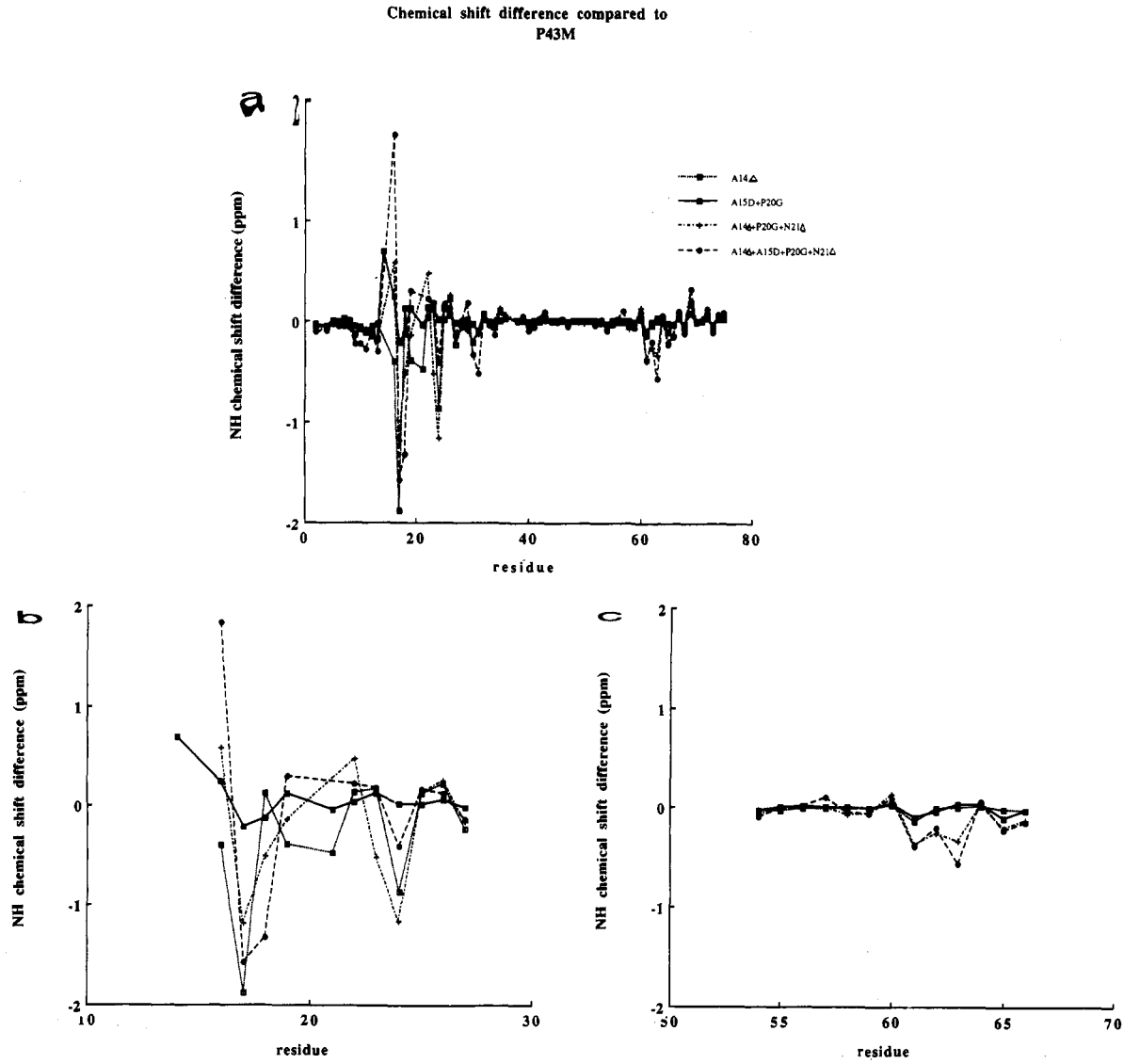

FIGURE 2: Chemical shift differences for amide protons of all mutant proteins compared to the mutant P43M: (a) all residues, (b) site 1, and (c) site 2.

also has a three-dimensional solution structure that closely resembles the crystal structure of the wild-type protein.

Assignments of the two mutants, A14Δ and A15D+P20G, were greatly simplified due to the many similarities with the mutant P43M and chemical shift differences are almost exclusively found for amino acids in loop 1(Figure 2). The chemical shift assignment could be obtained through comparison for 67 residues. The correctness of the sequential assignments was, however, always checked using the 200-ms NOESY spectra. For the other two mutants, A14Δ+P20G+N21Δ and A14Δ+A15D+P20G+N21Δ, larger shift differences were found in comparison with the P43M mutant. Most of the shift differences are still found for the amino acids in loop 1, but some residues in the end of loop 2 and in helix 4 also differ by more than ±0.1 ppm. Furthermore, deviations in the chemical shifts extend out from loop 1 into helix 2 much more than for the other two mutant proteins. Due to this, the majority of the amino acid residues for the regions above had to be sequentially assigned without reference to the other calbindins. Chemical shift differences between the four mutants and P43M are summarized in Figure 2, and the shift tables with the complete ^{1}H NMR assignments are given as supplementary material. Figure 2 shows that the curves of the chemical shift versus residue number divide the five mutants into two groups. The chemical shifts of P43M, A14Δ, and A15D+P20G are strikingly similar as are those of A14Δ+P20G+N21Δ and A14Δ+A15D+P20G+N21Δ. This suggests that the structures within each group are the same.

NH Exchange. The exchange rates for the backbone NH protons have been measured for the mutant A14Δ+A15D+P20G+N21Δ, and they are shown in Figure 3. The classifications of the NH protons as fast or slowly exchanging are almost identical to those of the wild-type protein (Kördel *et al.*, 1989). We therefore assume that the other mutant proteins also have unchanged NH exchange rates, since the studied mutant has the most extensive modifications. To correlate the exchange rates with the structure of the mutant protein the hydrogen bonds have been evaluated for the accepted conformations (supplementary material). This shows that when there is a strong hydrogen bond (hydrogen–donor distance less than 3.0 Å) existent in at least 50% of the conformations, the involved NH exchanges slowly, with some exceptions (D19, E35, F50, and E64). If, however, the hydrogen–acceptor distance is allowed to be 3.2 Å instead of 3.0 Å, even these four NHs participate in hydrogen bonds.

Global Fold. Structure calculations were carried out for two of the mutant proteins reported here, A15D+P20G and A14Δ+A15D+P20G+N21Δ. These two mutants were chosen for structure determination since one (A15D+P20G) has chemical shifts very similar to the wild-type, whereas the other

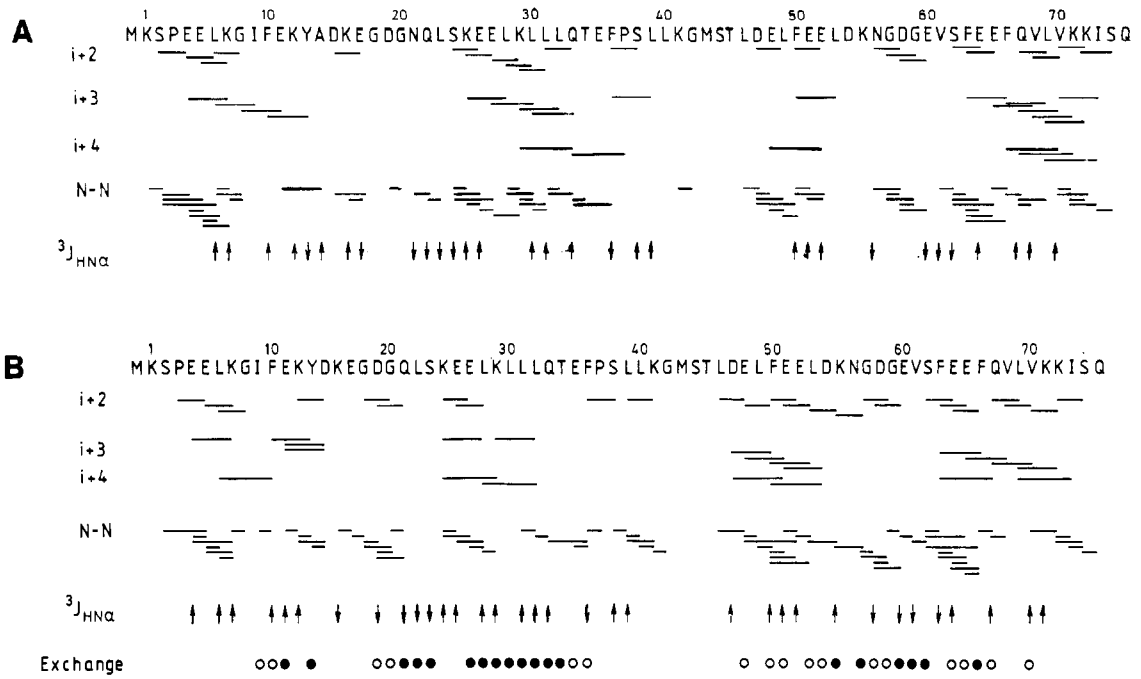

FIGURE 3: The medium range NOE connectivities. The one letter code for the amino acid sequence is given at the top. Characteristic NOE connectivities $d_{NN}(i,i+2)$, $d_{\alpha N}(i,i+2)$, $d_{\alpha N}(i,i+3)$, $d_{\alpha N}(i,i+4)$, $d_{\alpha\beta}(i,i+3)$, and all d_{NN} are indicated by lines between the two participating residues. Values of $^3J_{NH\alpha}$ are classified as small (<5 Hz) or large (>8 Hz) as indicated by an arrow up or down, respectively. Backbone amide protons that exchange slowly are indicated with solid circles and those exchanging neither fast nor slowly with open circles. Note that residues 14 and 21 are missing for the mutant A14Δ+A15D+P20G+N21Δ: (A) A15D+P20G and (B) A14Δ+A15D+P20G+N21Δ.

mutant differs to a greater extent. In the first calculations 793 (A15D+P20G) and 636 (A14Δ+A15D+P20G+N21Δ) distance constraints were included. In order to obtain the final conformations, five (A15D+P20G) and six (A14Δ+A15D+P20G+N21Δ) cycles of calculations (dg-SA-refinement) were needed. In each cycle 30 conformations were generated, and the best of these (30–50%) were analyzed to obtain new distance constraints and stereospecific assignments. The final number of constraints (804 and 654, respectively) and stereospecific assignments can be found in the supplementary material.

The distance constraints are unevenly spread over the amino acid residues (supplementary material) with few constraints per residue in the regions 15–20, 37–47, and 51–59 as well as in the C- and N-termini of the protein. Through comparison with the solution structure of the P43G mutant (Kördel *et al.*, 1993) and the secondary structure elements characterized by ^{1}H NMR assignments, it is clear that these regions correspond to the calcium-binding loop 1, linker region, and loop 2, respectively. Furthermore, the aromatic residues F10, F63, and F66 as well as L23, have by far the largest number of constraints/residue for both mutants. These residues in P43G are buried in the core of the protein with a multitude of possibilities of close contact with other protons.

Figure 3 shows the distribution of the specific distance constraints between NH-NH(i,i+2), NH-C$^\alpha$H(i,i+2), NH-C$^\alpha$H(i,i+3), NH-C$^\alpha$H(i,i+4), and C$^\alpha$H-C$^\beta$H(i,i+3). Strong NOE contacts between the protons listed above show the existence of α-helices (Wüthrich, 1986). Due to the high proportion of helices in calbindin the overlap in chemical shifts of NH, C$^\alpha$H, and C$^\beta$H is significant. It was therefore often difficult to unambiguously identify certain connectivities, especially $d_{\alpha\beta}(i,i+3)$. In spite of this, Figure 3 shows that both mutant proteins have four α-helices (residues 2–14, 24–36, 46–53, and 63–73), as is expected for a protein with two EF-hands. Moreover, these helices are structurally well defined, with the exception of helix 3. From the observation

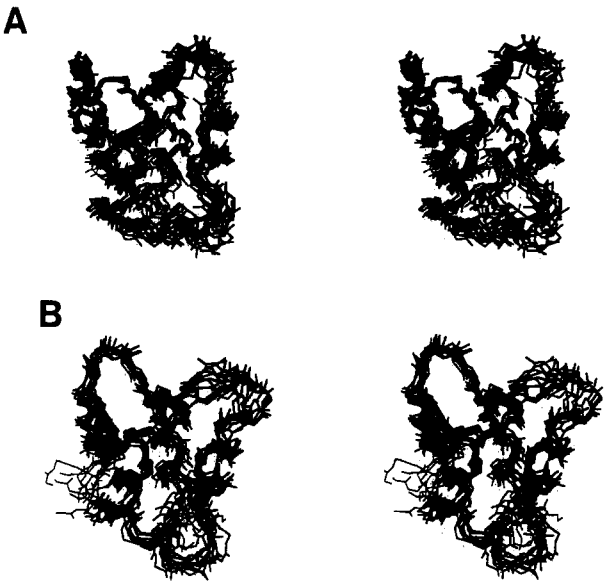

FIGURE 4: Stereoview of the backbone traces of 10 conformations for all amino acid residues: (A) A15D+P20G and (B) A14Δ+A15D+P20G+N21Δ.

of a few critical long range NOEs we conclude that the short β-sheet, normally found between the two Ca^{2+}-binding loops in a pair of EF-hands, is conserved for all five mutants.

With the final set of constraints (supplementary material) 120 conformations were generated in XPLOR for both mutant proteins. Out of these, 29 (A15D+P20G) and 24 (A14Δ+A15D+P20G+N21Δ) were accepted, and the backbone traces of 10 of these are shown in Figure 4a,b. It is apparent that the overall global folds of the structures of both mutants are the same and that the structures also are the same as for the mutant P43G (Kördel *et al.*, 1993). They all consist of two helix-loop-helix pairs with the calcium-binding loops (residues 14–27 and 54–65) connected by a short antiparallel β-sheet (residues 21–24 and 60–62) toward the ends of the loops.

Table I: rmsd Values from Comparison of the 29 (A15D+P20G) and 24 (A14Δ+A15D+P20G+N21Δ) Solution Structure Conformations of the Calcium-Loaded Mutants

residues	rmsd av	rmsd pairwise
	A15D+P20G	
back, 3–73	1.33	1.90+/–0.35
back, 2–36	0.72	1.04+/–0.25
back, 46–73	1.11	1.59+/–0.29
back, 2–14	0.65	0.93+/–0.24
back, 27–36	0.37	0.52+/–0.20
back, 46–54	0.89	1.23+/–0.44
back, 65–73	0.43	0.64+/–0.29
back, all except linker	0.99	1.42+/–0.21
back, loop 1, 14–27	0.62	0.91+/–0.44
back, loop 2, 54–65	0.98	1.40+/–0.34
all, 3–73	1.85	2.66+/–0.32
all, 2–36	1.25	1.80+/–0.25
all, 46–73	1.80	2.58+/–0.41
all, 2–14	1.17	1.68+/–0.31
all, 27–36	0.93	1.33+/–0.19
all, 46–54	1.57	2.19+/–0.46
all, 65–73	1.01	1.49+/–0.42
all, except linker	1.58	2.27+/–0.26
loop 1, 14–27	1.22	1.76+/–0.41
loop 2, 54–65	1.76	2.27+/–0.26
	A14Δ+A15D+P20G+N21Δ	
back, 3–73	1.29	1.87+/–0.31
back, 2–36	0.92	1.33+/–0.37
back, 46–73	1.43	2.05+/–0.44
back, 2–14	0.87	1.22+/–0.43
back, 27–36	0.56	0.81+/–0.23
back, 46–54	0.70	0.97+/–0.29
back, 65–73	0.64	0.88+/–0.35
back, all except linker	1.28	1.85+/–0.34
back, loop1 14–27	0.59	0.86+/–0.65
back, loop2 54–65	1.46	2.06+/–0.62
all, 3–73	1.74	2.51+/–0.28
all, 2–36	1.37	1.97+/–0.31
all, 46–73	1.88	2.70+/–0.43
all, 2–14	1.29	1.84+/–0.40
all, 27–36	1.14	1.64+/–0.20
all, 46–54	1.34	1.88+/–0.36
all, 65–73	1.18	1.68+/–0.36
all, except linker	1.70	2.45+/–0.29
all, loop1 14–27	1.24	1.81+/–0.55
all, loop2 54–65	2.06	2.92+/–0.64

When the helices are numbered 1–4 starting at the N-terminal α-helix , the overall structure is such that helix 1 (h1) is on one side of the molecule and h3 on the other, with h2 and h4 side-by-side between them (Figure 1c). All the consecutive helices are antiparallel. Furthermore, the two calcium-binding sites are situated on one side of the molecule opposite to the N- and C-termini together with the linker region (residues 37–45).

Root Mean Square Deviations. Root mean square deviations (rmsd) for different subsets of the molecule of both mutants are collected in Table I, showing the overall agreement of the conformations. The best determined regions in both mutants are the α-helices (e.g., helix 1, 0.65 Å; helix 2, 0.37 Å; for A15D+P20G), except helix 3. This is expected since these regions have the largest number of constraints/residue. Helix 3 consists only of two to three turns in the helix and is undetermined in the beginning, the region immediately following the linker region. Somewhat larger, but still low, rmsd values are obtained for the N-terminal half (residues 2–36) of the mutants, where the average rmsd is 0.72 (A15D+P20G) or 0.85 Å (A14Δ+A15D+P20G+ N21Δ) from the average position of the backbone atoms. The first half of both mutants is significantly better defined than the second half (residues 46–73), since the two regions with the highest rmsd, helix 3 and loop 2, belong to the latter. If nearly

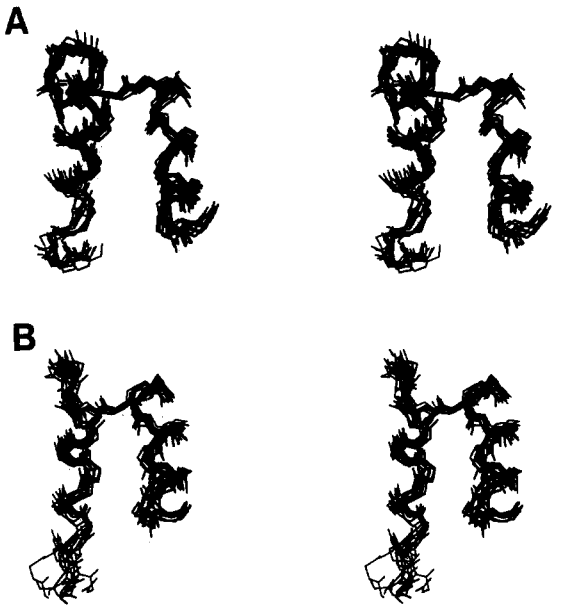

FIGURE 5: Stereoview of the backbone traces of 10 conformations of the N-terminal halves of the calcium-loaded proteins: (A) A15D+P20G and (B) A14Δ+A15D+P20G+N21Δ.

all backbone atoms are included (residues 2–73), the rmsd again is somewhat larger, 1.33 or 1.31 Å, respectively, for the two mutants. However, the goal of this project was to compare the fold of the first calcium-binding site in the two mutants with each other and with the wild-type protein. Therefore it is important to note that the N-terminal half with loop 1 (Figure 5) is one of the best determined regions in the proteins, making it very easy to draw conclusions concerning its fold.

Calcium-Binding Sites. The structure of A15D+P20G is essentially identical to the P43G mutant (Kördel *et al.*, 1993) in all regions, even in the calcium-binding sites (Figure 4). The solution structure of the wild-type protein has not been determined; however, the global fold of P43G and the wild-type are identical (Kördel *et al.*, 1990). The modifications in the calcium-binding site of A15D+P20G are thus not sufficient to achieve a change in the pseudo-EF-hand fold. Furthermore, judging from the close similarities in chemical shift of P43M, A14Δ, and A15D+P20G the structures of these other two mutants are also the same as that of the wild-type. Thus it is not enough to shorten the loop by one residue, as in A14Δ, to induce the site to turn inside-out and coordinate calcium by the side-chain carboxylates. Neither are the mutations in A15D+P20G sufficient to achieve a change in the pseudo-EF-hand fold. In A15D+P20G there is still an alanine in the first position of the loop and therefore the glycine will be in the seventh position and not the sixth position as in a normal EF-hand. In order for the aspartate to be the first amino acid to coordinate calcium, helix 1 would have to be rotated by $^1/_3$ of a turn to incorporate the extra amino acid. This is energetically unfavorable and thus not a very likely change. The backbone traces of the calcium-binding loops in the two mutants are drawn in Figure 6. The folds of site 1 in A15D+P20G and A14Δ+A15D+P20G+N21Δ are markedly different, whereas the folds of site 2 (the normal EF-hand), in both proteins are identical within the error limit, and they are also identical to site 1 in A14Δ+A15D+P20G+N21Δ. In the pseudo-EF-hand conformation there are constraints between the side chains of A14, A15, and G20, inducing the loop to wrap around the calcium ion. The normal EF-hand, loop 1 and 2 in A14Δ+A15D+P20G+N21Δ and loop 2 in A15D+P20G, however,

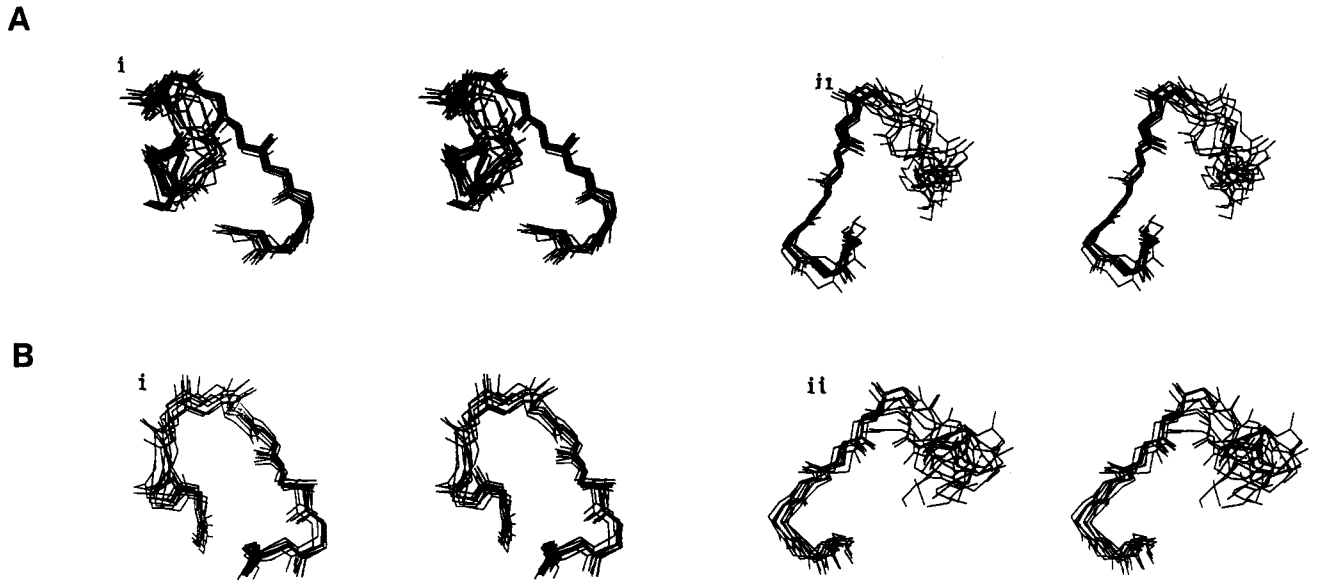

FIGURE 6: Stereoviews of the backbone traces of 10 conformations of the calcium-binding loops of the calcium-loaded proteins: (A) A15D+P20G and (B) A14Δ+A15D+P20G+N21Δ (i) site 1 and (ii) site 2.

FIGURE 7: Stereoview of the backbone traces of calcium-binding site 1 of A14Δ+A15D+P20G+N21Δ. Ten conformations of the solution structures (thin lines) are fitted to the crystal structure (thick line) by least-squares fitting of the backbone.

is much more open, and there are no constraints from the middle of the loop to the beginning. Figure 6 shows that in the mutant A14Δ+A15D+P20G+N21Δ we have succeeded in turning the mutated pseudo-EF-hand into a normal EF-hand, whereby the calcium ion is coordinated by side-chain carboxylates.

In a recent independent study A. L. Svensson (personal communication) has succeeded in crystallizing the mutant (A14Δ+A15D+P20G+N21Δ) and has determined its crystal structure. The first calcium-binding loop in both the solution and crystal structure of this mutant are shown overlaid in Figure 7. From this figure it is apparent that the fold of the site is the same in both the solution and crystalline state. Since NMR normally provides few distance constraints for such open structures as the calcium-binding loops, the side chains in the solution structures are not well-determined. On the other hand, in the crystal structure the side chains are as well defined as the rest of the molecule. The modified calcium-binding loop with the coordinating amino acids is shown in Figure 8 for the crystal structure, which shows that it is the side-chain carboxylates that coordinate calcium. These coordinating amino acids are oriented in the same way in the solution structure. However, due to the lack of constraints there is a spread in the side-chain conformations. Bearing in mind that site 1 is the same in both the solution and crystal state, it is clear that site 1 is a normal EF-hand. As a final proof, Figure 9 shows the overlaid structures of site 1 in A14Δ+A15D+P20G+N21Δ and site 2 in A15D+P20G, which is a normal EF-hand. Apart from the normal EF-hand

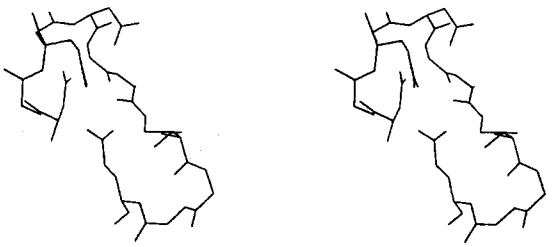

FIGURE 8: Stereoview of the calcium-binding site 1 in the crystal structure. The side chains of the residues that coordinate calcium are shown as well as the backbone trace.

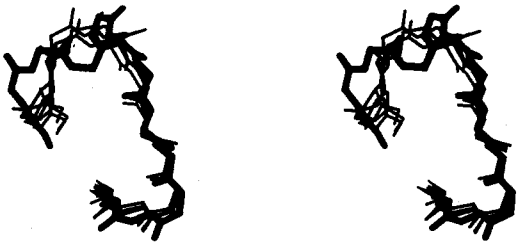

FIGURE 9: Stereoview of the backbone traces of calcium-binding site 1 of A14Δ+A15D+P20G+N21Δ and site 2 in A15D+P20G. Ten conformations of site 1 in A14Δ+A15D+P20G+N21Δ (thin lines) are fitted to site 2 in A15D+P20G (thick line) by least-squares fitting of the backbone.

having a rather high rmsd, which means that there is a spread in the conformations, the two overlaid sites are very similar.

As mentioned above the curves of the chemical shift versus the residue number (Figure 2) closely follow each other for A14Δ+P20G+N21Δ and A14Δ+A15D+P20G+N21Δ. We therefore believe that the mutations in A14Δ+P20G+N21Δ are sufficient to change the fold of site 1. Thus, it does not seem necessary to have aspartate in the first position of the loop for the site to adopt an EF-hand fold, as long as the loop is 12 amino acids long and there is a glycine in the sixth position. The calcium-binding constant to this site is low (Table II), however, compared to that in A14Δ+A15D+P20G+N21Δ, which probably is due to the missing aspartate. Putkey *et al.* (1989) have studied the inactive site in cardiac TnC, which has leucine in position 1. This site binds calcium with a very low binding constant, but when the leucine is mutated into an aspartate the calcium-binding becomes

Table II: Calcium-Binding Constants of the Five Mutant Proteins (Johansson *et al.*, 1990, 1991)

mutant	K_1 (M^{-1})	K_2 (M^{-1})
wild type	2.2×10^8	3.7×10^8
A14Δ	5×10^7	2×10^6
A15D+P20G	1.3×10^8	2.3×10^8
A14Δ+P20G+N21Δ	1.4×10^8	1×10^4
A14Δ+A15D+P20G+N21Δ	1.2×10^8	1.2×10^7

significant. These findings are in complete agreement with our results for the calbindin mutants.

Proline appears to be necessary for the pseudo-EF-hand to have a stiff loop. To be able to accommodate proline the loop must be lengthened by two amino acids. This induces the loop to turn inside-out and coordinate the calcium ion by the main-chain carbonyls. When the pseudo-EF-hand is left unmodified, the calcium dissociation rate (k_{off}) from the site is <10 s^{-1}, whereas when proline is removed and the fold is that of a normal EF-hand k_{off} increases to 6700 s^{-1} (Johansson *et al.*, 1991). From k_{off} and the calcium-binding constant (Johansson *et al.*, 1991), the association rate, k_{on}, can be calculated. For the mutant in which the fold of the site is changed (A14Δ+A15D+P20G+N21Δ) k_{on} is surprisingly high, 10^{10}–10^{11} M^{-1} s^{-1} as compared to 10^9 M^{-1} s^{-1} for the wild-type. This agrees well with the fact that the site now has become more open for the approach of the calcium ion.

CONCLUSIONS

The solution structures of two mutant proteins of calbindin D_{9k} show that the N-terminal Ca^{2+}-binding site in calbindin D_{9k} can accommodate either a pseudo-EF-hand fold, as in the wild-type protein, or an archetypal EF-hand, without altering the global fold of the protein. In the archetypal EF-hand the calcium-binding loop is 12 residues long, and calcium is coordinated by side-chain carboxylates from four residues (one bidentately), one backbone carbonyl, and one H_2O molecule. The pseudo-EF-hand loop is, however, prolonged by two amino acids, and the coordinating amino acids are different, thereby forcing the loop to turn inside-out and coordinate the calcium by five main-chain carbonyls, one side-chain carboxyl (bidentately), and one H_2O. The two mutant proteins have both been modified in the N-terminal site to try to change the fold of the pseudo-EF-hand into a normal EF-hand. In the mutant A14Δ+A15D+P20G+N21Δ we have succeeded with this, whereas the fold of the N-terminal site in A15D+P20G is unaltered. The solution structures as well as the ^1H NMR assignments for three additional mutant calbindins show that aspartate (position 1) is not critical for the fold of the loop. Previously we have found, however, that the aspartate is of utmost importance for the Ca^{2+} affinity. In the absence of this aspartate the Ca^{2+}-binding constant is too low to be of any physiological importance. Furthermore, according to results from ^{113}Cd NMR the loop in the N-terminal site can be a normal EF-hand fold, even though there is an extra amino acid in position 7 of the fold (Johansson *et al.*, 1991). This, however, modifies details of the fold and the strong hydrogen bond from the amide proton of glycine (position 6) to the carboxylate side chain of aspartate (position 1) cannot be formed. Finally shortening of the pseudo-EF-hand loop by one amino acid in the beginning of the loop does not change its fold. For the fold to change it is not sufficient to change alanine in position 2 into aspartate together with proline (position 7) into glycine, even though they are separated by five residues as in the normal EF-hand.

We thus conclude that it is possible to fit a normal EF-hand into the N-terminal site of calbindin D_{9k} and still retain both the calcium affinity and global fold of the protein.

ACKNOWLEDGMENT

We are grateful to Peter Drakenberg for making the MAGNE program available to us and to A. Svensson for making the crystal structure of the mutant calbindin available to us prior to publication. We are also grateful to Eva Thulin and Ingrid Andersson for the protein expression and purification and to Maria Sunnerhagen and Peter Sellers for helpful comments.

SUPPLEMENTARY MATERIAL AVAILABLE

Figures containing number of constraints versus residue number for A15Δ+P20G and A14Δ+A15Δ+P20G+N21Δ and tables of NOE constraints and stereospecific assignments, hydrogen bonds, and ^1H NMR chemical shifts (15 pages). Ordering information is given on any current masthead page.

REFERENCES

Ahomäki, T., Annila, A., & Drakenberg, T. Magnetic Moments.
Babu, Y. S., Sack, J. S., Greenhough, T. G., Bugg, C. E., Means, A. R., Babu, Y. S., Bugg, C. E., Cook, W. J. (1988) *J. Mol. Biol. 204*, 191–204.
Bax, A., & Davis, D. G. (1985) *J. Magn. Reson. 65*, 355–360.
Billeter, M., Braun, W., & Wüthrich, K. (1982) *J. Mol. Biol. 155*, 321–346.
Braunschweiler, L., Bodenhausen, G., & Ernst, R. R. (1983) *Mol. Phys. 48*, 535–560.
Braunschweiler, L., & Ernst, R. R. (1983) *J. Magn. Reson. 53*, 521–528.
Brodin, P., Johansson, C., Forsén, S., Drakenberg, T., & Grundström, T. (1990) *J. Biol. Chem. 265*, 11125–11130.
Brünger, A. T. (1990) XPLOR Manual v2.2, Yale University, New Haven, CT.
Chazin, W. J., & Wright, P. E. (1987) *Biopolymers 26*, 973–977.
Chazin, W. J., Rance, M., & Wright, P. E. (1988) *J. Mol. Biol. 202*, 603–622.
Chazin, W. J., Kördel, J., Thulin, E., Hofmann, T., Drakenberg, T., & Forsén, S. (1989) *Biochemistry 28*, 8646–8653.
Cook, W. J. (1985) *Nature 315*, 37–40.
Finn, B. E., Kördel, J., Thulin, E., Sellers, P., & Forsén, S. (1992) *FEBS 298*, 211–214.
Fullmer, C. S. (1992) *J. Nutr. 122*, 644–650.
Herzberg, O., & James, M. N. G. (1985) *Nature 313*, 653–659.
Herzberg, O., Moult, J., & James, M. N. G. (1986) *J. Mol. Biol. 261*, 8761.
Holroyde, M. J., Robertsson, S. P., Johnson, J. D., Solaro, R. J., & Potter, J. D. (1980) *J. Biol. Chem. 255*, 11688–11693.
Isobe, T., & Okuyama, T. (1978) *Eur. Jour. Biochem. 89*, 379–388.
Johansson, C., Brodin, P., Grundström, T., Thulin, E., Forsén, S., & Drakenberg, T. (1990) *Eur. J. Biochem. 187*, 455–460.
Johansson, C., Brodin, P., Grundström, T., Forsén, S., & Drakenberg, T. (1991) *Eur. J. Biochem. 202*, 1283–1290.
Johnson, J. D., Collins, J. H., Robertson, S. P., & Potter, J. D. (1980) *J. Biol. Chem. 255*, 9635–9640.
Karplus, M. (1963) *J. Am. Chem. Soc. 85*, 2870.
Kördel, J. (1991) Thesis.
Kördel, J., Forsén, S., & Chazin, W. J. (1989) *Biochemistry 28*, 7065–7074.
Kördel, J., Forsén, S., Drakenberg, T., & Chazin, W. J. (1990) *Biochemistry 29*, 4400–4409.
Kördel, J., Skelton, N. J., Akke, M., & Chazin, W. J. (1993) *J. Mol. Biol.*, in press.
Kraulis, P. J. (1991) *Jour. Appl. Cryst. 24*, 946–950.

Kretsinger, R. H. (1987) *Cold Spring Harbor Symposium on Quantitaive Biology*, Vol. LII, pp 499–510.
Kretsinger, R. E., Mann, J. E., & Simmonds, J. G. (1982) In *Proceedings of the Fifth Workshop on Vitamin D* (Norman, A. W., Ed.) pp 233–248, De Gruyter, New York.
Levine, B. A., & Williams, R. J. P. (1982) In *Calcium and Cell Function* (Cheung, W. J., Ed.) Vol. 2, pp 1–38, Academic Press, New York.
Linse, S., Brodin, P., Drakenberg, T., Thulin, E., Sellers, P., Elmdén, K., Grundström, T., & Forsén, S. (1987) *Biochemistry 26*, 6723–6735.
Linse, S., Johansson, C., Brodin, P., Grundström, T., Drakenberg, T., & Forsén, S. (1991) *Biochemistry 30*, 154–162.
Macura, A., & Ernst, R. R. (1980) *Mol. Phys. 41*, 95–117.
Marion, D., & Wüthrich, K. (1983) *Biochem. Biophys. Res. Commun. 113*, 967–974.
Pardi, A., Billeter, M., & Wüthrich, K. (1984) *J. Mol. Biol. 180*, 741–751.
Putkey, J. A., Sweeney, H. L., & Campbell, S. T. (1989) *J. Biol. Chem. 264*, 12370–12378.
Rance, M. (1987) *J. Magn. Reson. 74*, 557–564.
Shaka, A. J., Lee, C. J., & Pines, A. (1988) *J. Magn. Reson. 77*, 274–293.
Skelton, N. J., Kördel, J., Forsén, S., & Chazin, W. J. (1990) *J. Mol. Biol. 213*, 593–598.
States, D. J., Haberkorn, R., & Ruben, D. (1982) *J. Magn. Reson.* 286–292.
Strynadka, N. C. J., & James, M. N. G. (1989) *Annu. Rev. Biochem. 58*, 951–998.
Sundralingam, M., Bergstrom, R., Strasburg, G., Rao, S. T., Roychowdhury, R., Greaser, M., & Wang, B. C. (1985) *Science 227*, 945–948.
Svensson, A. L., Thulin, E., & Forsén, S. (1992) *J. Mol. Biol., 223*, 601–606.
Szebenyi, D. M. E., Obendorf, S. F., & Moffat, K. (1981) *Nature 294*, 327–332.
Szebenyi, D. M. E., & Moffat, K. (1986) *J. Biol. Chem. 261*, 8761–8777.
van Eerd, J.-P., & Takahashi, K. (1976) *Biochemistry 15*, 1171–1180.
Vogel, H. J., Drakenberg, T., Forsén, S., O'Neil, J. D. J., & Hofmann, T. (1985) *Biochemistry 24*, 3870–3876.
Wagner, G. (1983) *J. Magn. Res. 55*, 151–156.
Wagner, G., Braun, W., Havel, T. F., Schaumann, T., Go, N., & Wütrich, K. (1987) *J. Mol. Biol. 196*, 611–639.
Wnuk, W., Schoechlin, M., & Stein, E. A. (1984) *J. Biol. Chem. 259*, 9017–9023.
Wüthrich, K. (1986) *NMR of Proteins and Nucleic Acids*, Wiley, New York.